

V-Potential Double Layers and the Formation of Auroral Arcs

J. S. Wagner, T. Tajima,^(a) J. R. Kan, J. N. Leboeuf,^(a) S.-I. Akasofu, and J. M. Dawson^(b)

Geophysical Institute, University of Alaska, Fairbanks, Alaska 99701

(Received 19 November 1979)

A simulation study of the electrostatic interaction of a field-aligned electron current sheet with ambient hot ions ($T_e/T_i \approx 0.6$) and a conducting boundary shows that a V-shaped potential double layer spontaneously develops and accelerates electrons to the ion thermal energy. It is proposed that this double-layer process is responsible for the aurora energy supply. Only as T_e/T_i approaches unity, the potential exceeds T_i via resistivity enhanced by wave trapping of electrons.

PACS numbers: 52.25.Lp, 94.30.Kq, 52.65.+z

The acceleration mechanism of electrons which cause the polar aurora has been one of the most challenging problems in cosmic electrodynamics. Satellite observations reveal two intriguing features associated with thin curtainlike auroral forms (auroral arcs) surrounding the geomagnetic pole. The first is that an auroral arc is caused by a thin sheet of electrons streaming down along geomagnetic field lines and these electrons carry a significant amount of field-aligned (upward-directed) current.¹ The second is an indication that the sheet current is associated with a V-shaped potential structure in which a potential difference of a few kilovolts is present along the geomagnetic field lines above the auroral ionosphere.² Several mechanisms, including double layers and anomalous resistivity, have been proposed for sustaining such a field-aligned potential difference in a collisionless plasma (see review³).

On the basis of the present simulation study, the following physical picture has emerged in an attempt to explain the above observations. A magnetized sheet of current-carrying electrons and hot shielding ions (of plasma sheet origin) is injected through a cool background plasma towards a conducting (ionospheric) boundary. As the hot ions try to shield the current sheet, a potential drop forms perpendicular to the magnetic field as a result of their larger Larmor radius (the potential contours being parallel to the magnetic field). The partially shielded electron beam approaches the conducting boundary and is accelerated towards it, because the electrons near the boundary "see" their opposite charged images on the other side of the boundary. As the electron sheet beam reaches the conductive layer, the potential contours close, forming a V-shaped potential structure. The resulting potential drop is limited by the ion kinetic energy T_i , in agreement with a two-dimensional, double-layer solution to Poisson's equation for a steady-state con-

dition.⁴

However, once the electrons become accelerated, they excite electrostatic waves through the two-stream instability under certain conditions, and they become trapped in the waves. When this occurs, the total potential drop results from the interaction potential (limited by T_i) and anomalous resistivity (unlimited by T_i). Thus, the double layer develops through a two-step process, involving both the conducting boundary and the anomalous resistivity. The backscattered electrons play a crucial role in that without them the double layer is not stable and the collisionless plasma is unable to sustain a steady-state voltage drop. Ionospheric electrons and backscattered electrons are supplied from the lower boundary to guarantee overall charge neutrality. Note that this is in contrast with the formation of a classical sheath where the plasma gains potential with respect to the wall because electrons are depleted because of their higher thermal velocity and are lost from the plasma.

Our simulation shows that not only does a double-layer solution exist, but it forms spontaneously and remains stable provided that the proper initial and boundary conditions are met. This is the first two-dimensional simulation that shows a double layer can form under auroral conditions, and demonstrates that it is capable of accelerating the current-carrying electrons to the observed energies.

The initial and boundary conditions which we use are (i) an upper boundary through which current-carrying electrons and hot magnetospheric ions are supplied from the plasma sheet, (ii) a lower conducting boundary through which the upstreaming ionospheric ions and the trapped electrons are supplied (the ionospheric Pederson and Hall conductivities are much larger than those in the magnetosphere), and (iii) a cool background plasma.

Electrons and ions are injected at a constant rate (drift velocity V_{e1} and temperature T_e and T_i) from the upper magnetospheric boundary ($x = N_x \Delta$ with Δ being the grid size, the x axis parallel to the field lines). Similarly, ionospheric ions are supplied at a constant rate from the lower boundary ($x = 0$) from half-Maxwellian reservoirs, but the injection of trapped electrons is varied in order to maintain overall charge neutrality. Because of this variation, and because particles are allowed to leave the system through either boundary, the current is not determined by the particle sources at the boundary. However, when the double-layer potential becomes large enough to reflect upstreaming electrons and downstreaming ions between the double layer and the boundaries, the current is controlled by the electron source and the upstreaming ions. The potential drop⁵ along field lines is not applied, but is allowed to evolve self-consistently as a result of the interaction. This is different from many previous double-layer simulations⁶ in

which the potential was imposed externally.

The simulation is carried out according to a bounded $2\frac{1}{2}$ dimensional electrostatic algorithm⁷: periodic in the y direction, and bounded in the x with the potential $\varphi = 0$ specified at $x = 0$ (the conducting boundary) and $E_x = 0$ at $x = N_x \Delta$. The current-carrying electrons are magnetized and remain as a sheet of finite thickness l_y immersed in hot ions. At $x = 0$, downstreaming electrons are reflected up by degrading the energy by 6%. The reflected electrons are to simulate backscattering of the energy-degraded primary electrons, which we find to play an important role in the formation of the V -potential double layer. Typical parameters employed are grid size $N_x \times N_y = 128 \times 32$, $l_y = 6\Delta$, the particle number 32 768, $V_{e1} = 0.76v_{e1}$, where v_{e1} denotes electron thermal velocity, the electron cyclotron and plasma frequencies $\Omega_e = 2\omega_{pe}$, the mass ratio $m_i/m_e = 10$, and the electron Debye length $\lambda_{De} = \Delta$.

Figure 1 shows the potential structure, the electron and ion phase spaces at $t = 2500\omega_{pe}^{-1}$. [Fig-

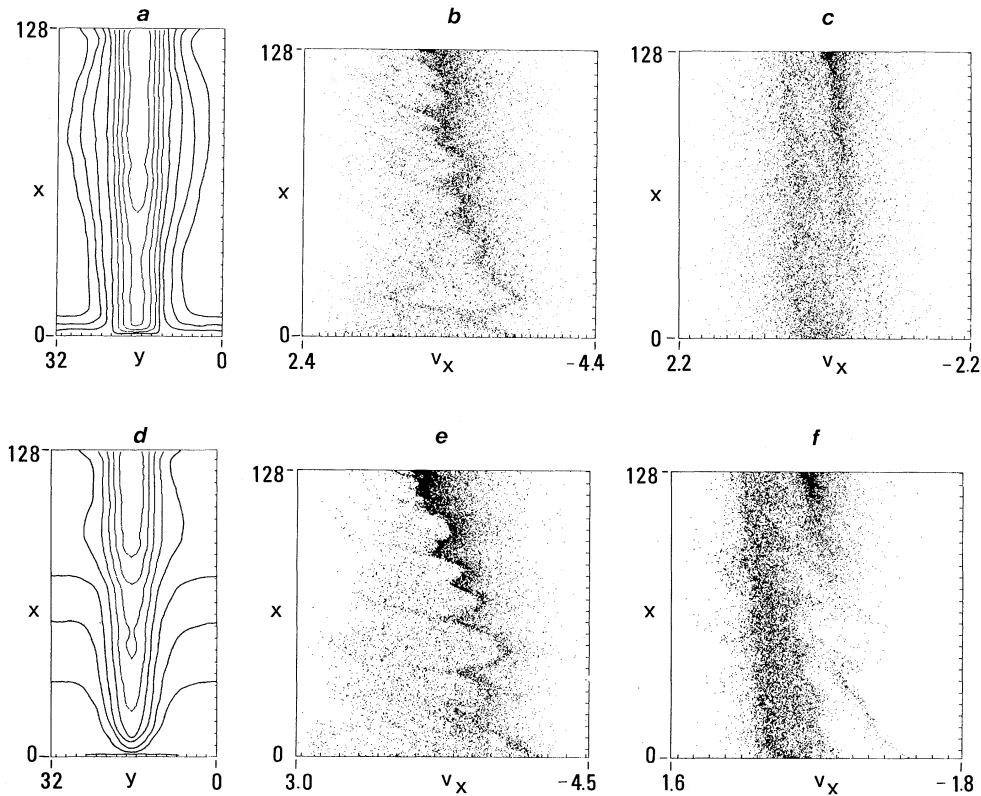


FIG. 1. Stable double layer at $t = 2500\omega_{pe}^{-1}$. (a)-(c) $T_e/T_i = 0.2$; (d)-(f) $T_e/T_i = 0.6$. (a) Potential contours with spacing $\Delta\varphi = 0.07T_i$. $\varphi = 0$ at $x = 0$. (b) Electron phase space, integrated over y as in (c), (e), and (f). (c) Ion phase space. (d) Potential contours with $\Delta\varphi = 0.25T_i$. $\varphi = 0$ at $x = 0$. (e) Electron phase space. (f) Ion phase space.

ures 1(a)–1(c) for the case with temperature ratio $T_e/T_i = 0.2$, while (d)–(f) for a cooler ion case with $T_e/T_i = 0.6$.] The temperature ratio $T_e/T_i = 0.2$ closely models magnetospheric conditions. A clear field-aligned potential drop is observed in both cases. A double-layer structure is evident in the ion and electron phase spaces for both sequences. In time, the double-layer structure approaches steady state around $75\omega_{pe}^{-1}$, and remains for the length of the run (up to $2500\omega_{pe}^{-1}$).

The potential for the case $T_e/T_i = 0.2$ shows that the majority of the potential drop ($0.7T_i$) occurs over a short distance of $6\lambda_{De}$ near and above the conducting boundary (the ionosphere). Above this steep gradient the potential increases slowly (an additional $0.06T_i$) over a length of about $L \sim 60\lambda_{De}$. This additional potential is small compared to the drop near the conducting boundary. In the double-layer region, there are downstreaming electrons, trapped electrons (by the double layer), upstreaming ions, and trapped ions.

For $T_e/T_i = 0.6$, the potential increases from zero to T_i over a distance of $7\lambda_{De}$ and then continues to increase at a slower rate, but to considerably higher energy ($21T_i$) over a distance of $100\lambda_{De}$. This suggests that there are two complementary mechanisms which produce the total potential drop when the T_e/T_i ratio increases toward unity. The first mechanism occurs only within $\sim 7\lambda_{De}$ and the potential is limited by the ion kinetic energy; this is the same for the case $T_e/T_i = 0.2$. The second mechanism operates when T_e approaches or becomes greater than T_i . Associated with this “additional potential drop” is the prominent electron trapping by large amplitude electrostatic waves as seen in Fig. 1(e). These waves are due to the Buneman instability excited by the accelerated electrons. Since the most unstable wave number $k \sim \omega_{pe}/V_e(x)$ changes as the electron beam is accelerated, the electron phase space modulation wavelength increases as the beam propagates toward the conducting boundary. The wavelength of the vortex structure can be scaled approximately by $\lambda(x) = 2\pi V_e(x)\omega_{pe}^{-1}$. The trapping of electrons by these waves can lead to an increase of the effective resistivity (anomalous electron dragging⁸) and thus contributes to the additional voltage drop distributed over the length where the instability is active.

The effective collision frequency associated with the additional voltage drop as a function of the temperature ratio T_e/T_i is shown in Fig. 2(a). The effective collision frequency ν_e^* is determined by the effective conductivity $\sigma^* = \omega_{pe}^2/4\pi\nu_e^*$,

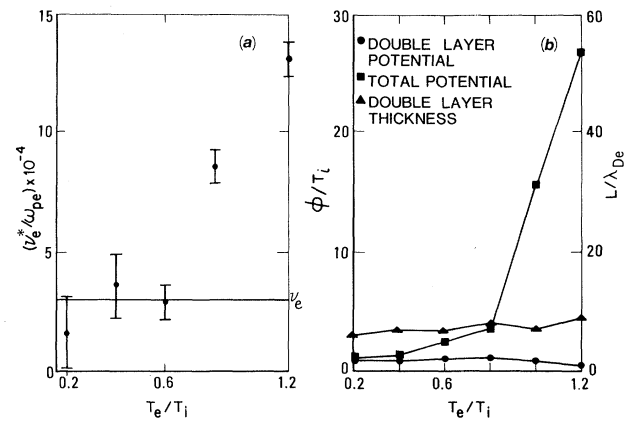


FIG. 2. (a) Effective resistivity in the double layer for various T_e/T_i . (b) Structure of the double layer at various T_e/T_i .

where the conductivity is measured by electronic current density divided by the electric field at the location where the additional drop takes place. When T_e/T_i reaches about 1, the effective collision frequency becomes well over the level given by normal collisions ν_e . Figure 2(b) indicates that the two-dimensional double-layer potential provides approximately the same amount of voltage drop ϕ/T_i irrespective of T_e/T_i . The total voltage drop ϕ/T_i across the system, however, increases as T_e/T_i increases. At the same time, the V-shaped equipotential lines become more and more straight horizontal stripes, i.e., one-dimensional structure. For larger temperature ratios (T_e/T_i), it is easier to overcome the threshold of the Buneman instability as well as those of the ion-acoustic and ion-cyclotron instabilities.

The present simulation of the two-dimensional V-potential double layer reproduces many of the features which are found in the formation of auroral arcs. The essential elements include a field-aligned electron sheet current interacting with the surrounding magnetospheric ions and the conducting ionosphere. The stable two-dimensional double layer accelerates electrons to the energy of the ambient hot ions in agreement with the observations¹ for the case of $T_e/T_i \sim 0.2$ which is reasonable in the plasma sheet. In this temperature-ratio regime $T_e/T_i \leq 0.6$, the contribution of anomalous resistivity to the acceleration of electrons is not important [see Fig. 2(a)]; it becomes important when $T_e/T_i \geq 0.6$. The tendency of increasing potential drop in the double layer for increasing field-aligned electron velocity V_{e1} (see Fig. 3) is also consistent with auroral observa-

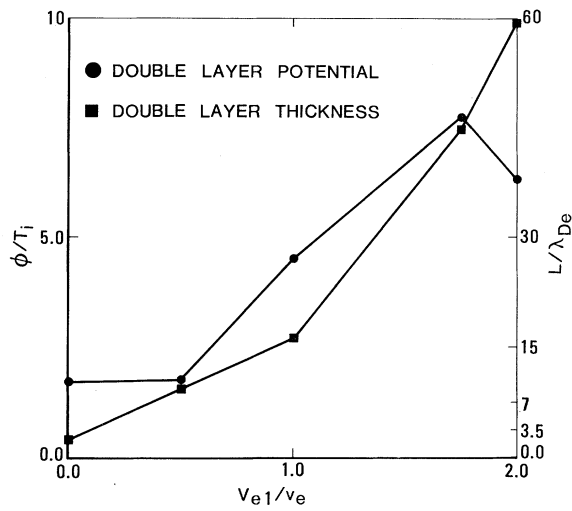


FIG. 3. Properties of the double layer as a function of electron drift velocity V_{e1} .

tions: A brighter aurora is associated with a higher intensity of the field-aligned current. When the temperature ratio is fixed at $T_e/T_i = 0.2$, the structure stays as Vshaped even when V_{e1} is increased; the length of the double layer is found to be proportional to V_{e1} .

This work was supported in part by the National Science Foundation Grants No. ATM 79-16470 and No. ATM 78-19253.

^(a)Also at Physics Department, University of California, Los Angeles, Cal. 90024.

^(b)Permanent address: Physics Department, University of California, Los Angeles, Cal. 90024.

¹R. L. Arnoldy, P. B. Lewis, and P. O. Issacson, *J. Geophys. Res.* **79**, 4208 (1974).

²F. S. Mozer, C. W. Carlson, M. K. Hudson, R. B. Torbert, B. Parody, Y. Yatteau, and M. C. Kelley, *Phys. Rev. Lett.* **38**, 292 (1977).

³C.-G. Fälthammar, *Rev. Geophys. Space Phys.* **15**, 457 (1977).

⁴J. R. Kan, L. C. Lee, and S.-I. Akasofu, *J. Geophys. Res.* **84**, 4305 (1979).

⁵C. Goertz and G. Joyce, *Astrophys. Space Sci.* **32**, 165 (1975).

⁶J. S. DeGroot, C. Barnes, A. E. Walstead, and O. Buneman, *Phys. Rev. Lett.* **38**, 1283 (1977); R. F. Hubbard and G. Joyce, *J. Geophys. Res.* **84**, 4297 (1979).

⁷V. K. Decyk and J. M. Dawson, *J. Comput. Phys.* **30**, 407 (1979).

⁸J. N. Leboeuf, T. Tajima, and J. M. Dawson, *Phys. Rev. Lett.* **43**, 1321 (1979).